Climate Dynamics
https://doi.org/10.1007/s00382-018-4228-x

An inter-decadal increase in summer sea level pressure over the Mongolian region around the early 1990s

Haiyan Zhang[1,3] · Zhiping Wen[1,2,5] · Renguang Wu[4] · Xiuzhen Li[1,5] · Ruidan Chen[1,5]

Received: 26 October 2017 / Accepted: 27 April 2018

Abstract
The East Asian summer monsoon is affected by processes in the mid-high latitudes in addition to various tropical and subtropical systems. The present study investigates the summer sea level pressure (SLP) variability over northern East Asia (NEA) and emphasizes the closed active center over the Mongolian region. It is found that the seasonal mean Mongolian SLP (MSLP) anomaly is closely connected with the variability of summertime regional synoptic extra-tropical cyclones on longer time scales. A significant inter-decadal increase in the MSLP around the early 1990s has been detected, which is accompanied by a weakening in the activity of regional extra-tropical cyclones. Recent warming over NEA may have a contribution to the inter-decadal change, which features evidently meridional inhomogeneity around 45°N. The inhomogeneous air temperature anomaly distribution results in decreased vertical wind shear, reduced atmospheric baroclinicity over the Mongolian region, and thus inactive regional cyclones and increased MSLP in the latter decade. The associated temperature anomaly distribution may be partly attributed to regional inhomogeneity in cloud and radiation anomalies, and it is further maintained by two positive feedback mechanisms associated with atmospheric internal processes: one via adiabatic heating and the other via horizontal temperature advection.

Keywords SLP variability over the Mongolian region · Synoptic extra-tropical cyclones · Inhomogeneous warming

1 Introduction

The East Asian summer monsoon (EASM) is a unique and complex subsystem of the Asian climate system. On one hand, it is affected by various tropical and subtropical systems, such as the western North Pacific subtropical high, the East Asian Meiyu front, tropical cyclones and intraseasonal oscillations (Ye and Zhu 1958; Zhu et al. 1986; Tao and Chen 1987; Chen et al. 2001, 2015; Mao and Chan 2005; Wang and Chen 2008; Tong et al. 2009; Lu et al. 2014). On the other hand, the EASM subjects to the impact of synoptic processes in the mid-high latitudes (Tao 1980; Zhou et al. 2003) among which one dominant feature is migratory cyclonic circulation systems and associated fronts. In comparison, fewer studies have been conducted about the impacts of synoptic systems on seasonal mean change in the EASM.

Extra-tropical cyclones are often accompanied by strong winds, temperature and pressure changes. As they move southward, dry and cold airs invade into southern China, which may induce abnormal precipitation there. Climatologically, one of the regions with most frequent occurrence of extra-tropical cyclones is the Mongolian region (Chen et al. 1991; Wang et al. 2009; Zhang et al. 2012). Many studies have focused on the influences of synoptic cyclones on temperature, rainfall and dust storm in China (Watts 1969; Zhang 1989; Qian et al. 2002; Liu et al. 2003). Some studies, on the other hand, have documented the linkage between circulation anomalies over northern East Asia (NEA) and the

✉ Zhiping Wen
zpwen@Fudan.edu.cn

1 Center for Monsoon and Environment Research, School of Atmospheric Sciences, Sun Yat-sen University, Guangzhou, China

2 Institute of Atmospheric Sciences, Fudan University, Shanghai 200433, China

3 South China Sea Marine Forecasting Center of State Oceanic Administration, Beijing, China

4 Center for Monsoon System Research, Institute of Atmospheric Physics, Chinese Academy of Sciences, Beijing, China

5 Jiangsu Collaborative Innovation Center for Climate Change, Nanjing, China

Published online: 10 May 2018

EASM on the inter-annual time scale. Wu and Zhang (2011) revealed that the third leading EASM mode obtained by the complex vector empirical function analysis was characterized by two distinct and alternating modes, one of which featuring a cyclonic/anticyclonic anomalous wind field at 850-hPa over NEA. Zhao and Zhou (2005) defined a zonal thermal contrast index using the difference of surface pressure between Mongolia and the western North Pacific to depict the year-to-year variability of monsoon, which could epitomize the EASM intensity and the variability of summer rainfall along the Yangtze River. Lin and Wang (2016) identified that an intensified summer low over northern continental East Asia (EA) may induce decreased rainfall over NEA and South China and enhanced rainfall along the Huai River valley.

The inter-decadal variability of climate has drawn great attentions during the past decades, which is one of the research foci in climate variability and predictability. In recent years, some studies have revealed that large-scale sea and land surface thermal conditions experienced notable changes around the early 1990s. There was more frequent and persistent occurrence of the El Niño Modoki events since then (Weng et al. 2007). The North Atlantic sea surface temperature became warmer (Li and Bates 2007). The sea surface temperature anomaly in the Indo-Pacific warm pool switched from a cold phase to a warm phase around the mid-1990s, even after the removal of a warming trend (Wang and Mehta 2008). The spring sensible heat flux and snow depth over the Tibetan Plateau decreased over the period between 1980 and 2008 (Duan et al. 2013). Under these backgrounds, the EASM system underwent a remarkable inter-decadal change. The change featured a large increase in precipitation over southern China around 1993, including parts of the Yangtze River basins and South China (Ding et al. 2008; Lei et al. 2011; Liu et al. 2011; Zhu et al. 2014). Wu et al. (2010) proposed that two anomalous lower-tropospheric anticyclones were vital to the inter-decadal change in southern China precipitation: one over the South China Sea–western North Pacific, and the other over NEA. The outflows from these two anticyclones converged over southern China, leading to enhanced moisture convergence, anomalous ascent, and increased rainfall. Zhang et al. (2017) found that an equivalent barotropic anticyclonic circulation anomaly over NEA was one of the most robust characteristics for the inter-decadal change in the EASM around the early 1990s. As the anticyclonic anomaly over NEA is an important aspect for the above inter-decadal change, unravelling plausible causes for its occurrence may help to improve understanding of the change in the EASM.

In analyzing the summer sea level pressure (SLP) variability over NEA, we noticed a significant increase in the Mongolian SLP (MSLP) around the early 1990s, which was consistent with the anomalous anticyclone over NEA mentioned above. Some possible explanations for this change were proposed. Wu et al. (2010) argued that it may be related to an increase in the Tibetan Plateau snow cover in the preceding winter–spring, which led to a contrast in temperature change between the plateau and the surrounding regions, and the development of high surface pressure. Zhu et al. (2012) suggested that the increased surface air temperature around the Lake Baikal generated an anomalous lower-tropospheric anticyclone over NEA, which was further demonstrated by numerical simulations (Du et al. 2016). It is found that recent warming over NEA exhibits evidently spatial inhomogeneity (refer to their Fig. 7). Is it possible that the inhomogeneous warming makes a contribution to the inter-decadal increase in the MSLP? If so, what is the related physical process? These questions are worthy of investigation.

The organization of the paper is as follows. The datasets and analysis methods used in the present study are described in Sect. 2. Section 3 defines a MSLP anomaly index and investigates its connection with the activity of regional extratropical cyclones. Section 4 presents the inter-decadal variation of the MSLP and explores the plausible role of recent inhomogeneous warming over NEA. Finally, the summary and some discussions are given in Sect. 5.

2 Data and methodology

The primary data used in the present study are derived from the European Centre for Medium-Range Weather Forecasts (ECMWF) latest Reanalysis (ERA-Interim; Dee et al. 2011) on 2.5° ×2.5° global grids for the period 1979–2012, which includes summer (June–July–August, JJA) monthly mean SLP, skin temperature, horizontal winds, vertical velocity, geopotential height, and air temperature at 17 vertical pressure levels. The daily mean (arithmetic mean of 0000 and 1200 UTC) fields from ERA-Interim are also used. The monthly mean total cloud cover and surface net shortwave radiation are obtained from the National Centers for Environmental Prediction (NCEP)/Department of Energy (DOE) Global Reanalysis 2 (NCEP-2; Kanamitsu et al. 2002). This dataset is available on a 1.9° × 1.9° grid starting from January 1979. The convention for surface shortwave radiation is positive for downward radiation.

The empirical orthogonal function (EOF) analysis is performed to derive the spatio-temporal variations of summer SLP over NEA. The Mann–Kendall abrupt change test (Magaritz and Goodfriend 1987) is used to examine the inter-decadal variability of the MSLP. Composite analysis is applied to analyze atmospheric circulation anomalies associated with the inter-decadal variation of the MSLP. The Student's t test is employed to examine the significance

of composite anomalies. The harmonic analysis is used to extract the components of variations on specific periods.

An objective method is needed for identification of extra-tropical cyclones. Previous studies have put forward various identification methods based on minima in SLP or maxima in lower-tropospheric vorticity. The former is better at capturing the low-frequency margin, while the latter is focused more on the high-frequency end of synoptic range (Ulbrich et al. 2009). Referring to König et al. (1993) and Serreze (1995), the present analysis adopts a combination of pressure and vorticity based methods using the daily mean fields: (1) the SLP at a particular grid point is smaller than values at eight surrounding grid points, which means the existence of a closed low-pressure center; (2) the SLP at the central grid point is less than a defined threshold; (3) the area-mean 850-hPa relative vorticity over the 5°×5° box around the central grid is larger than 10^{-5} s^{-1}. The SLP threshold mentioned above varies with position. At a particular grid point, it is defined as the summer mean value (Fig. 1a) minus the standard deviation of synoptic components (whose period is shorter than 10 days) during recent 34 summers. The selection of the vorticity threshold value is somewhat subjective.

Some cyclone systems may have more than one sub centers on a particular day. In that case, we retain only the strongest one within 5° whose SLP is the minimum. Furthermore, we retain only the migratory cyclone systems so that the local continental warm thermal lows are excluded in counting cyclone centers. In this study, only extra-tropical cyclones centered within the region of 40°–60°N and 80°–140°E are concerned, as the Tibetan Plateau (20°–40°N and 60°–110°E) is such a tremendous topography that cyclones seldom occur over there (Wu 2002). The intensity

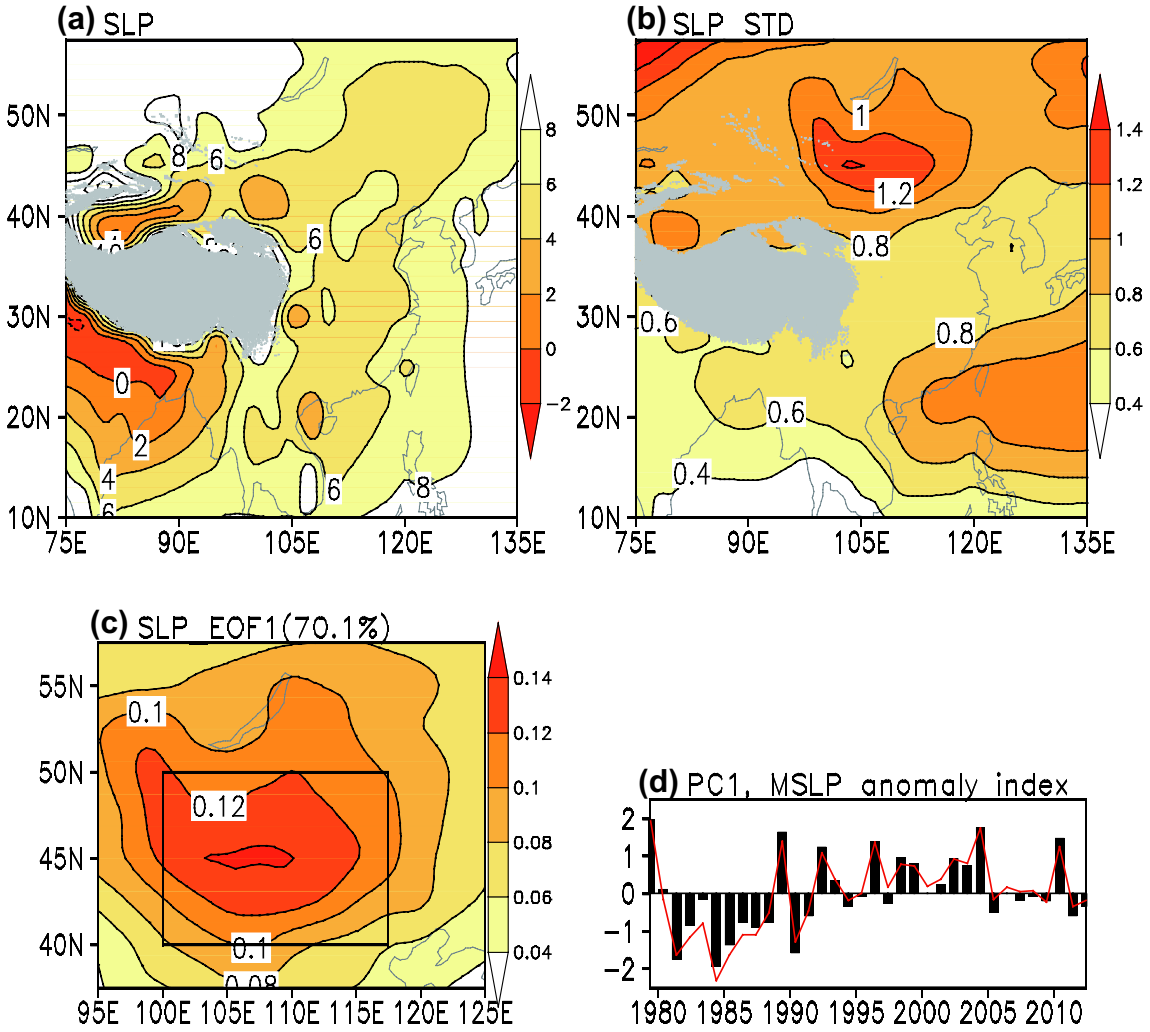

Fig. 1 **a** Climatological mean (unit: 1000 + hPa) and **b** standard deviation (unit: hPa) of summer SLP during 1979–2012. **c** Spatial pattern of the first leading EOF mode of northern East Asian SLP anomalies. **d** Time series of the normalized first principal component (PC1, black bar) and the MSLP anomaly index (red curve), which is defined as area-mean SLP anomalies over the region of 40°–50°N and 100°–117.5°E [boxed area in **c**]

of an extra-tropical cyclone is defined by its lowest center value of SLP. A similar method is applied to identify extra-tropical anticyclones, which requires an existence of a closed high-pressure center and a core vorticity less than $-1\times10^{-5}\ s^{-1}$. The related SLP threshold at a particular grid point is defined as the climatological SLP plus the standard deviation of synoptic components during recent 34 summers.

Extra-tropical cyclones owe their existence primarily to the baroclinicity of atmosphere. Following Hoskins and Valdes (1990), the baroclinicity is measured by the Eady growth-rate maximum which represents the growth rate of the most rapidly growing disturbances. It is calculated as

$$\sigma_{BI} = 0.31f\left|\frac{\partial\vec{V}}{\partial z}\right|N^{-1} \tag{1}$$

where f is the Coriolis parameter, N the Brunt–Väisälä frequency, $\vec{V}$ the horizontal wind speed, and z the vertical height. As seen from Eq. (1), the change of baroclinicity is closely related to the vertical wind shear and the Brunt–Väisälä frequency that is an indicator of the static stability of atmosphere. Both factors are linked to the air temperature anomalies. The vertical wind shear is proportional to the horizontal temperature gradient as

$$\frac{\partial\vec{V}}{\partial z} \cong \frac{g}{fT}\vec{K}\times\nabla T \tag{2}$$

where g is the gravitational acceleration and T the air temperature. The Brunt–Väisälä frequency is related to the vertical temperature distributions in the form of

$$N = \left(\frac{g}{\theta}\frac{d\theta}{dz}\right)^{1/2} \tag{3}$$

where θ is the potential temperature. On the basis of above formulas, the vertical wind shear, Brunt–Väisälä frequency, and baroclinicity are calculated at 17 vertical levels for period 1979–2012 using the ERA-Interim monthly datasets.

The thermodynamic equation in the isobaric coordinate system can be written as

$$\frac{\partial T}{\partial t} = -u\frac{\partial T}{\partial x} - v\frac{\partial T}{\partial y} - \left(\frac{p}{p_0}\right)^{R/C_P}\omega\frac{\partial\theta}{\partial p} + \frac{Q}{C_p} \tag{4}$$

where T is the air temperature, p the pressure, $p_0 = 1000$ hPa, R the universal gas-constant, C_p the specific heat of dry air at constant pressure,θ the potential temperature, and Q the diabatic heating. The left side of the equation is the local change rate of air temperature. The four terms on the right side represent the contributions of the zonal temperature advection, meridional temperature advection, vertical temperature advection, and external heating, respectively. The present study applies the thermodynamic equation to diagnose thermodynamic processes associated with the inhomogeneous warming over NEA.

3 Definition of the MSLP anomaly index and its connection with the activity of regional extra-tropical cyclones

Asia is controlled by large-scale thermal low near surface during summer, of which the strongest part is located in India (Fig. 1a). Apart from the Indian region, north China–Mongolia is another center of the Asian continental low featuring a southwest–northeast-elongated low-pressure belt. The minimum SLP as low as 1000 hPa is detected over northwestern China, which may be related to the terrain there. Due to its geographical location, the seasonal mean low depression over Mongolia was referred to as the summer Mongolian low (Zhao and Zhou 2005). Figure 1b presents the standard deviation of summer SLP. A striking closed active center with a maximum standard deviation of 1.4 hPa is observed over NEA. This indicates that the SLP there exhibits strong year-to-year variability.

An EOF analysis is performed on the SLP anomalies over the NEA domain (37.5°–57.5°N, 95°–125°E) to obtain the spatial pattern of SLP variations. The first mode explains about 70.1% of the total variance for the period 1979–2012. This mode is statistically distinguished from higher modes according to the rule of North et al. (1982). As shown in Fig. 1c, the first mode features a same sign variation over the whole domain with larger loading near Mongolia (~45°N). This distribution resembles closely that of the standard deviation in Fig. 1b. The corresponding principal component (PC1) is displayed in Fig. 1d (black bar), which shows a remarkable variability. Based on the distribution of the standard deviation and the loading of the first mode (Fig. 1b, c), we define a MSLP anomaly index using area-mean summer SLP anomalies over the Mongolian region (refer to the region of 40°–50°N, 100°–117.5°E in the present study if there is no extra instruction). The time series of the normalized MSLP anomaly index is shown in Fig. 1d (red line) for comparison. These two curves almost overlap with each other with a correlation coefficient of +0.98. It means that the MSLP anomaly index can represent well the major mode of SLP variability over NEA. This presents an important reason why the present study focuses on the SLP anomaly over the Mongolian region on the inter-annual and inter-decadal timescales, which has been less concerned compared to its synoptic to seasonal variations.

Located in the mid-high latitudes, disturbances in the Mongolian region are predominant on synoptic time scales. We perform a power spectral analysis to analyze the periods of daily MSLP during each summer for the period

1979–2012. There is a significant power at synoptic time scales with periods shorter than 10 days for most of the years (figure not shown). One dominant feature of mid-high latitudes synoptic processes is the frequent occurrence of extra-tropical cyclones. Although spring is the season when cyclones occur most frequently, cyclones are observed often in summer as well (Wang et al. 2009). Figure 2a displays the spatial distribution of long-term mean frequency of occurrence of summertime extra-tropical cyclones in NEA. A nearly southwest–northeast-elongated cyclone zone is observed with a maximum center over Mongolia, whose position is almost consistent with the seasonal mean Mongolian low in Fig. 1a. Synoptic anticyclones may occur in the extra-tropics as well (Chung and Dulam 2004), especially in the areas west to the Lake Baikal (Fig. 2b). However, the frequency of occurrence of anticyclones in the Mongolian region (about 6.1 days per year) is much less than that of cyclones (29.2 days per year, which is calculated by summing long-term mean frequency at all grid points within the region), which accounts for nearly one-third of the total days in summer. It is conceivable that the accumulation of synoptic extra-tropical cyclones contributes more to the seasonal mean MSLP. Therefore, the summer MSLP is mainly a macroscale manifestation of regional synoptic extra-tropical cyclone activity.

The activity of Mongolian cyclones (extra-tropical cyclones centered within the Mongolian region) displays strong year-to-year variability. Figure 3 presents the Mongolian extra-tropical cyclone frequency (METCF) index defined by total number of cyclones occurred within the Mongolian region during JJA in each year (Fig. 3a, red curve), as long as the Mongolian extra-tropical cyclone intensity (METCI) index defined by seasonal mean of intensity of these extra-tropical cyclones (Fig. 3b, blue curve). A positive value of the METCI anomaly index corresponds to a year with weakened Mongolian cyclones. Both the METCF and METCI index exhibit evident variability, with a standard deviation of 10.6 days and 0.76 hPa, respectively. It is expected that the Mongolian extra-tropical cyclone activity is closely related to the variation of seasonal mean SLP. The summer SLP over the Mongolian region tends to be below normal in the years when there are more and stronger regional cyclones during JJA. The correlation coefficient between the METCF and the MSLP anomaly index is −0.79, which is statistically significant at the 99.9% confidence level. Their correlation coefficients reach −0.56 and −0.94 on inter-annual and inter-decadal time scales, respectively. It indicates that the METCF index is highly related to the seasonal mean MSLP on both time scales. The METCI time series also show a significant correlation coefficient of

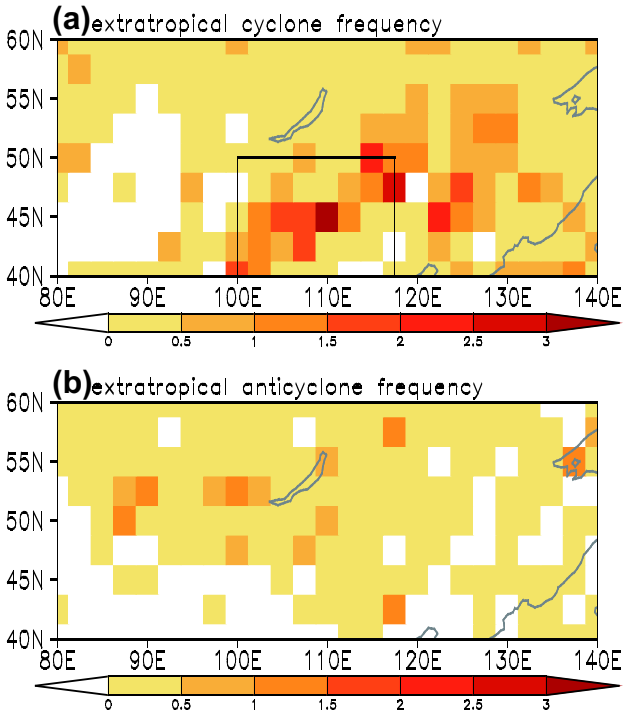

Fig. 2 **a** Spatial distribution of long-term mean frequency of occurrence (unit: days) of summertime extra-tropical cyclones as calculated at each grid point in NEA. **b** As in **a**, but for the frequency of occurrence of extra-tropical anticyclones

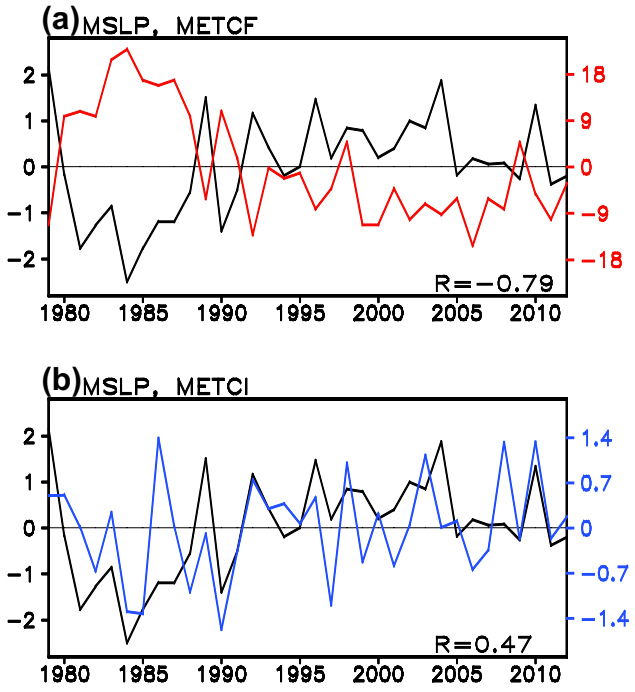

Fig. 3 Time series of anomalous **a** METCF index (red curve, unit: days) and **b** METCI index (blue curve, unit: hPa). The black curves denote the MSLP anomaly index. The numbers in the bottom denote the correlation coefficient between the METCF and the MSLP, and that between the METCI and the MSLP, respectively

+0.47 with the MSLP anomaly index. The seasonal mean MSLP anomaly may serve as a simple index to describe the variability of summertime synoptic Mongolian cyclones on loner time scales. Some external factors may lead to summer atmospheric circulation anomalies that in turn affect the occurrence of extra-tropical cyclones, which will be discussed later.

4 Inter-decadal variation of the MSLP and plausible role of inhomogeneous warming over NEA

4.1 An inter-decadal change around the early 1990s

As shown above, the MSLP exhibits evident variability (Figs. 1d, 3). Particularly, the MSLP seems to undergo an inter-decadal change around the early 1990s. Negative SLP anomalies are predominant prior to this time and positive anomalies are predominant after it, indicating an increase in the MSLP. To further confirm this change, the Mann–Kendall test for abrupt change has been conducted, and the result is shown in Fig. 4a. The intersection of UF and UB curves appears in 1990, indicating that 1990 is the time of the abrupt change. Figure 5 shows the mean SLP during 1980–1990 and 1991–2012 (denoted as epoch I and II, respectively) and the difference between these two periods. An obvious southwest–northeast-elongated low-pressure belt over north China–Mongolia is observed in both periods, but the summer low pressure becomes much weaker in the later decade. Robust positive SLP differences appear over the Mongolian region. The mean MSLP is 1004.4 hPa in epoch I and 1005.9 hPa in epoch II. The difference reaches 1.5 hPa, which is close to its standard deviation and is statistically significant at the 99.9% confidence level (Table 1).

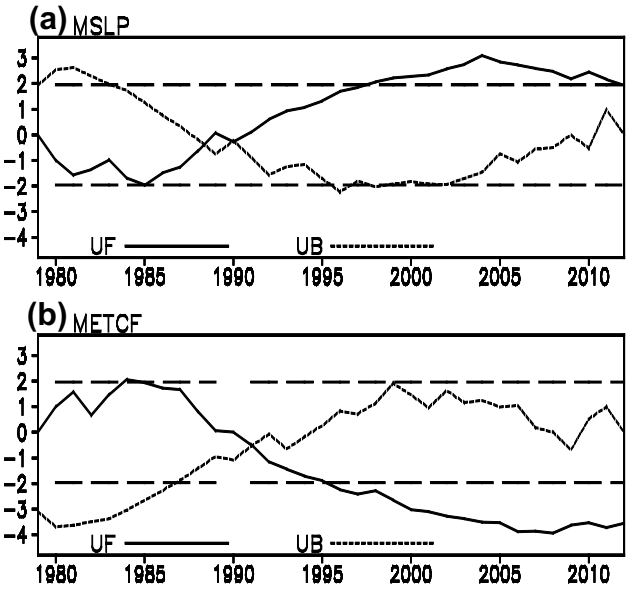

Fig. 4 **a** Curves for Mann–Kendall abrupt change coefficients UF and UB, based on the time series of MSLP anomaly index. The area between the two dashed lines indicates that the abrupt changing-point exceed the 95% confidence level. **b** As in **a**, but for results based on the time series of METCF index

As discussed above, the MSLP anomaly is closely connected with the activity of regional synoptic extra-tropical cyclones. Consistently, an inter-decadal change in the METCF around the early 1990s is identified (Fig. 4b). Figure 6 displays the number of days with cyclones at each grid point in epoch I and II separately along with the differences between the two decades. It is evident that the counts of extra-tropical cyclones are much less in epoch II, especially around 45°N (Fig. 6c). As shown in Table 1, the frequency of occurrence of Mongolian cyclones decreases by 18.2 days and the average core SLP increases by 0.5 hPa in the later decade, which are statistically significant according to the Student's t test. The accumulation of less and weaker Mongolian cyclones in epoch II is conducive to the increased MSLP. This is confirmed by the difference of mean SLP averaged over the Mongolian extra-tropical cyclone days between the two decades (figure not shown), whose spatial pattern is akin to that in Fig. 5c.

4.2 Plausible role of inhomogeneous warming over NEA

In the previous subsection, it has been revealed that the inter-decadal increase in the MSLP around the early 1990s is a robust feature and it is closely connected with the synoptic cyclone activity in the Mongolian region. In this subsection, we will explore related mechanisms for the change via understanding why there is inter-decadal change in the daily cyclone activity. Particularly, the possible role of recent warming over NEA is concerned. Figures 7 and 8 illustrates temperature differences between epoch II and epoch I, and their associations with the increase of MSLP.

The skin temperature over EA is generally warmer in the latter decade (Fig. 7). The regional warming exhibits evident inhomogeneity in the spatial pattern. The most robust warming area is located in the Lake Baikal region (~50°N), with the maximum warming exceeding 2 K. Much smaller temperature anomalies are observed over the adjacent Inner Mongolia Plateau of China (~40°N). Thus, there is an apparent contrast in temperature change between the two regions. Such a meridionally-inhomogeneous distribution of temperature anomalies extends to the lower troposphere below the pressure level of 600 hPa, as indicated by the vertical structure of air temperature change (Fig. 8a). According to the thermal wind balance [Eq. (2)], this temperature anomaly distribution results in a decrease in the lower-tropospheric

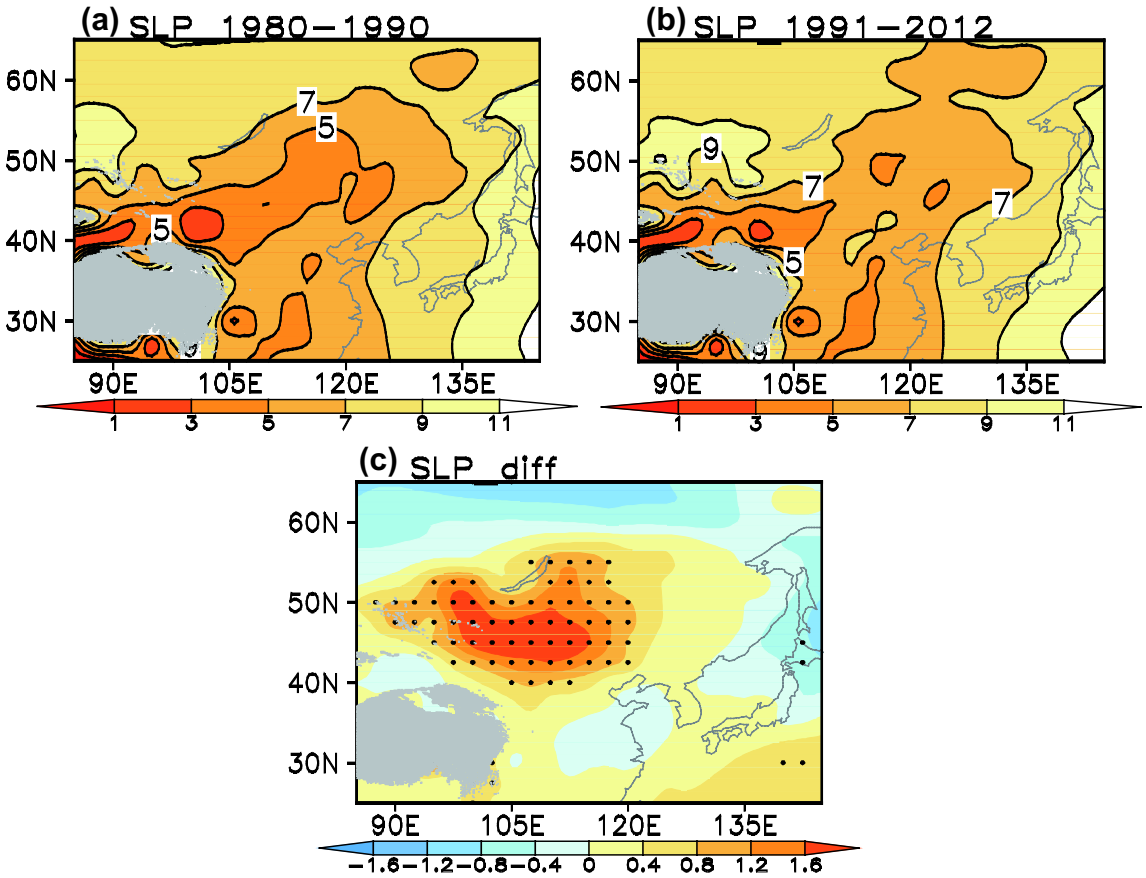

Fig. 5 Summer mean SLP (unit: 1000 + hPa) averaged over **a** 1980–1990 and **b** 1991–2012, and the difference between these two periods (**b** minus **a, c**; unit: hPa). The black dots in **c** denote the differences exceeding the 95% confidence level based on the Student's t test

Table 1 Decadal mean of summertime MSLP, METCF and METCI during 1980–1990 and 1991–2012 and the differences between the two periods

	MSLP (units: hPa)	METCF (units: days)	METCI (units: hPa)
1980–1990	1004.4	41.7	996.9
1991–2012	1005.9	23.5	997.4
Difference	1.5 (99.9%)	− 18.2 (99.9%)	0.5 (90%)

The percentage in brackets denotes the level of confidence of the inter-decadal change

vertical wind shear over the Mongolian region where the isotherms are most crowded (Fig. 8b). On the other hand, air temperature warming is uneven in the vertical direction, particularly over the areas north of 45°N where the surface warms faster than the mid-troposphere (Fig. 8a). This leads to a significant decrease in the lower-tropospheric static stability (Fig. 8c).

According to Eq. (1), both the vertical wind shear and static stability can contribute to the change in atmospheric baroclinicity. The baroclinicity tends to be strengthened when the wind shear increases and the stability decreases. As indicated by Fig. 8d, the distribution of atmospheric baroclinicity anomaly shows a good agreement with that of the change of vertical wind shear. It suggests that the decadal weakening of baroclinicity over Mongolia may be mainly explained by the decreased vertical wind shear, which is associated with the meridionally-inhomogeneous warming. The contribution of the decreased static stability is negligible. This point is further confirmed by the time series of anomalous lower-level vertical wind shear and atmospheric baroclinicity over the Mongolian region, both of which weaken synchronously since the early 1990s (figure not shown). Reduced baroclinicity impedes the genesis and development of regional synoptic extra-tropical cyclones. Thus, the Mongolian cyclone activity becomes less active in the later decade, and the mean MSLP increases as its macroscale manifestation (Fig. 3; Table 1).

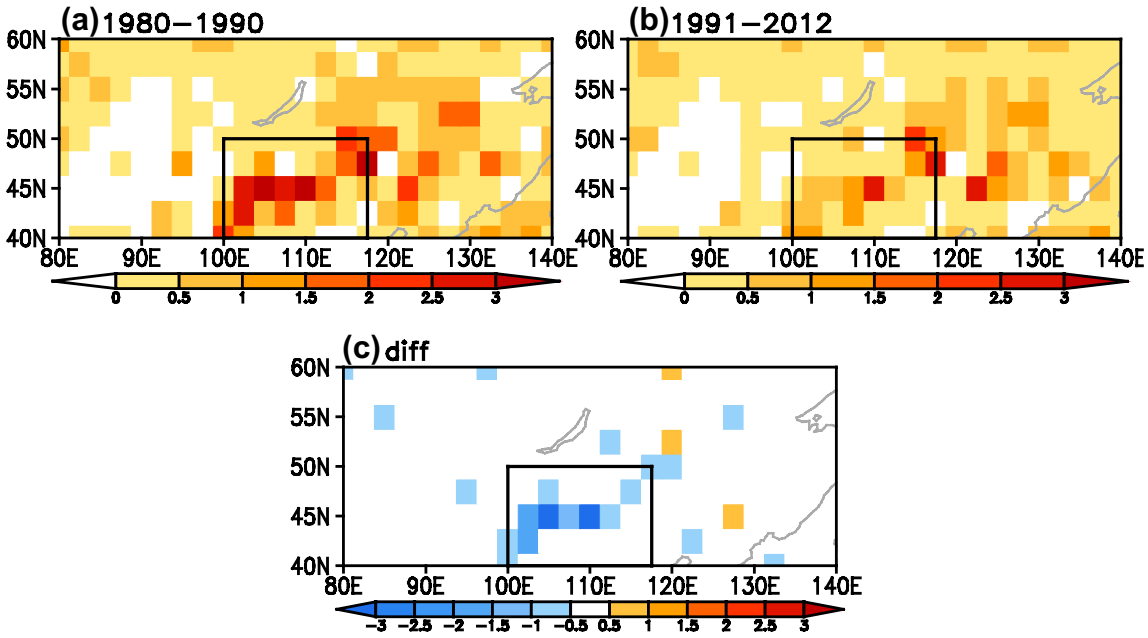

Fig. 6 Frequency of occurrence (unit: days) of summertime extra-tropical cyclones at each grid point averaged over **a** 1980–1990 and **b** 1991–2012, and the difference between the two periods (**b** minus **a, c**)

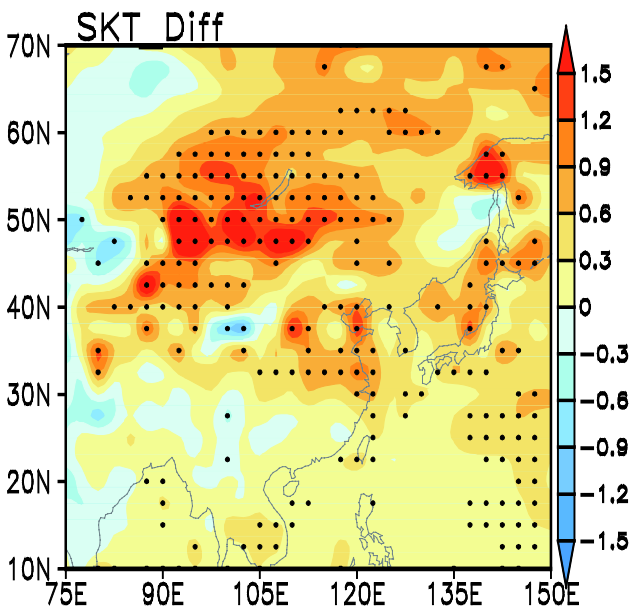

Fig. 7 Difference of the 1991–2012 mean minus 1980–1990 mean summer skin temperature (unit: K). The black dots denote the differences exceeding the 95% confidence level based on the Student's t test

The above analyses explain the inter-decadal increase in the MSLP from the change of background for the synoptic Mongolian cyclone using the monthly mean data. We have also examined inter-decadal anomalies of daily temperature and atmospheric circulation corresponding to the cyclone days over Mongolia. It is found that, over NEA that is the main domain of focus in this study, related results are generally equivalent to those based on monthly mean data (figure not shown). Thus, it is conceivable that the inhomogeneous inter-decadal warming of seasonal mean temperature contributes to inter-decadal change in the daily cyclone activity, which further contributes to the increase in the MSLP.

An additional question follows: what are responsible for the inhomogeneous warming? It may be partly attributed to the global warming with a robust center around the Lake Baikal, which is associated with the increase of greenhouse gases (Zhu et al. 2012). Besides, regional inhomogeneous distributions of cloud and radiation anomalies may have a contribution. Figure 9 shows that there are significantly less cloud and more incoming shortwave radiation over the areas north of 45°N during the post-1990s period compared to the former period (Fig. 9a, b), which can contribute to the local skin-surface warming (Fig. 7). In contrast, weak changes in surface net shortwave radiation are seen over the Inner Mongolia Plateau south of 45°N (Fig. 9b), which slows down the surface warming and leads to a meridionally-inhomogeneous temperature anomaly distribution (Fig. 7). Such a temperature anomaly distribution may extend upward to the mid-lower troposphere through turbulent heating (Fig. 9c, d).

Apart from the external forcing, the change in air temperature is affected by atmospheric internal processes. We analyze the circulation anomalies associated with the inter-decadal variation of the MSLP and find that the increased MSLP is accompanied by regional anomalous descent, with

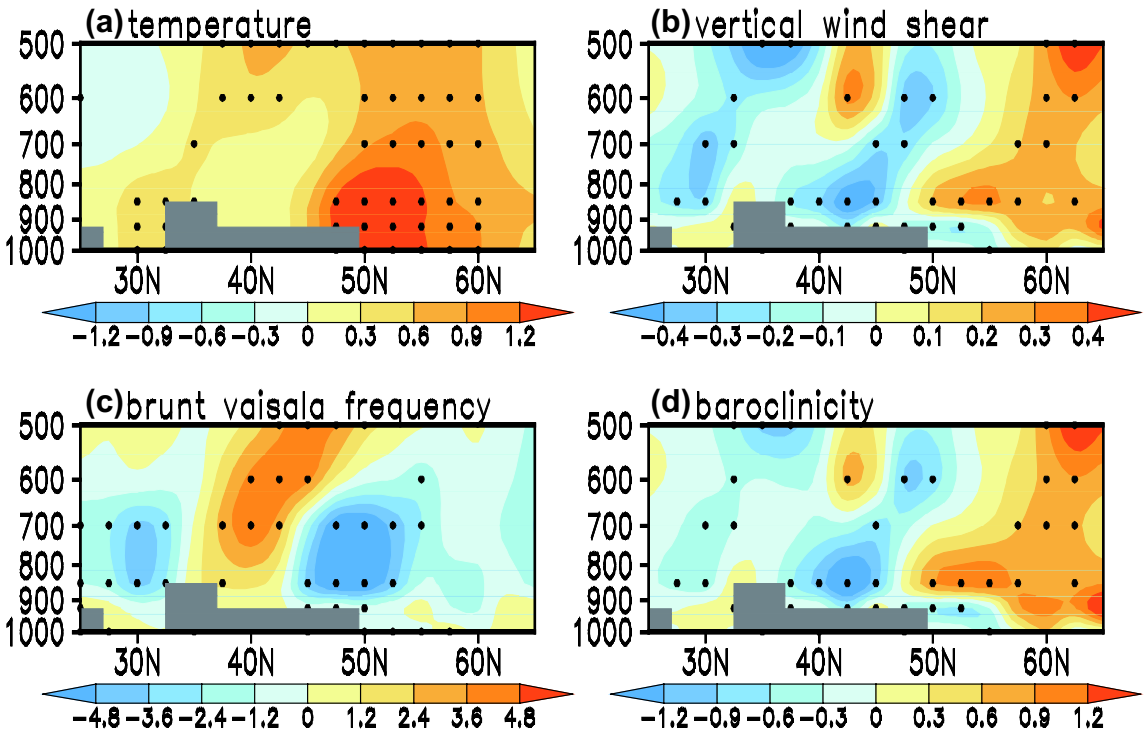

Fig. 8 Latitude-vertical sections of the difference between 1991–2012 and 1980–1990 mean summer **a** air temperature (unit: K), **b** vertical wind shear (unit: -1×10^{-2} m s^{-1} hPa^{-1}), **c** Brunt Vaisala frequency (unit: 10^{-3} s^{-1}) and **d** atmospheric baroclinicity (unit: day^{-1}) along 105°E. The black dots denote the differences exceeding the 95% confidence level based on the Student's t test

the strongest sinking around the Lake Baikal (Fig. 10a). This descent can lead to warmer temperature through adiabatic heating. The vertical warm temperature advection anomalies at 700 hPa are observed to be consistent with the sinking (Fig. 10b), which favors more rapid warming over the Lake Baikal region than over the areas to the south. It helps to maintain the meridionally-inhomogeneous temperature anomaly structure, which may result in the decadal increase in the MSLP in epoch II as discussed above. These processes form a positive feedback mechanism.

Another positive feedback mechanism is involved in maintaining the temperature anomaly distribution, which is related to horizontal temperature advection. Associated with the decadal increased MSLP, a pronounced lower-tropospheric anticyclone anomaly occupies NEA (Fig. 10c, the 850 hPa pattern is similar to that at 700 hPa and is thus omitted). Anomalous northeasterly/northerly winds prevail on the southeast flank of the anticyclone. Climatologically, the air temperature is low in the northeast and high in the southwest (Fig. 10c, color shading). Taking the mean temperature distribution into consideration, the northeasterly/northerly flow can cause anomalous cold advection over the Inner Mongolia Plateau south of 45°N (Fig. 10d). Figure 11 illustrates the changes in horizontal temperature advection in more detail. For both zonal and meridional temperature advection differences, significantly cold advection anomalies are observed over the Inner Mongolia Plateau, and their magnitudes are equivalent (Fig. 11 b, d). Both of them contribute to the anomalous horizontal cold advection there. The zonal cold advection anomalies are mainly attributed to the configuration of significantly easterly anomalies as strong as 2.8 m s^{-1} and the mean zonal temperature gradient (Fig. 11a) for the zonal temperature gradient differences are inconspicuous over south Mongolia (figure not shown). The meridional cold advection anomalies are mainly generated by anomalous northerly flow in the presence of the remarkable mean meridional temperature gradient, which can reach -6×10^{-6} K m^{-1} over Mongolia (Fig. 11c). The anomalous horizontal cold advection acts against the anomalous adiabatic heating over the Inner Mongolia Plateau region (Fig. 10b, d) and favors the formation of meridionally-inhomogeneous temperature anomalies.

5 Summary and discussion

In boreal summer, a southwest–northeast-elongated low-pressure belt is a remarkable feature over north China–Mongolia, which is one center of the Asian thermal low. Analyses show that the SLP over the Mongolian region exhibits strong year-to-year variability. The MSLP anomaly can depict the major mode of SLP variability over NEA which

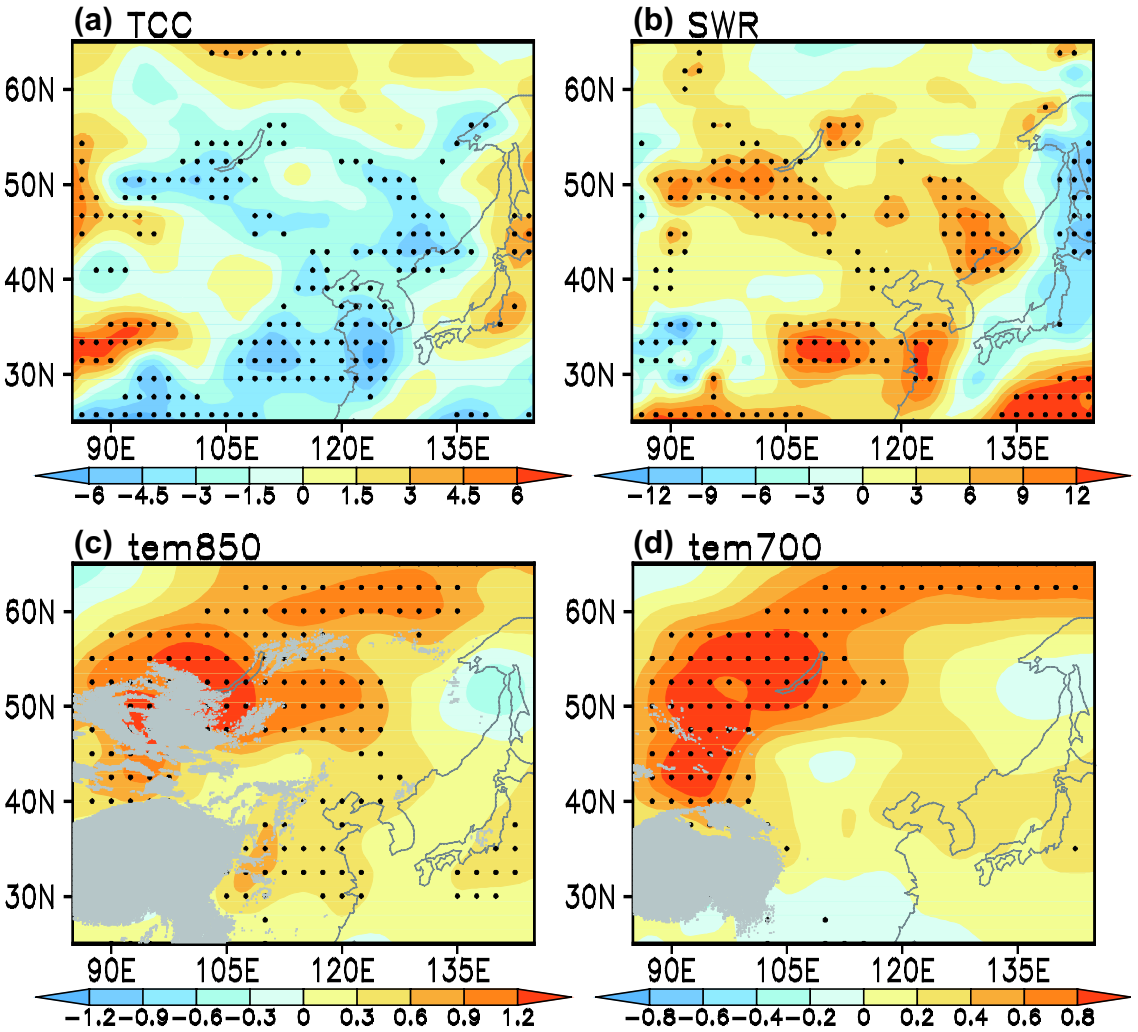

Fig. 9 Difference of the 1991–2012 mean minus 1980–1990 mean summer **a** total cloud cover (unit: %), **b** surface net shortwave radiation (unit: W m^{-2}), and air temperature (unit: K) at **c** 850 hPa and **d** 700 hPa. The black dots denote the differences exceeding the 95% confidence level based on the Student's t test

features a same sign variation. This presents a scientific significance of studying the MSLP anomaly on the inter-annual and inter-decadal timescales, which has been less concerned compared to its synoptic to seasonal variations.

The present study reveals that there is frequent concurrence of synoptic extra-tropical cyclones along the seasonal mean low-pressure belt. And the MSLP anomaly index can reflect the year-to-year variability of regional synoptic cyclones. The summer SLP tends to be below-normal in the years when there are more and stronger Mongolian cyclones, and vice versa. Thus, the seasonal mean MSLP anomaly may serve as a simple index to describe the variability of summertime Mongolian cyclones on longer time scales without identification of individual synoptic systems.

The present study detects a robust inter-decadal increase in the MSLP around the early 1990s, which is consistent with previous studies (Wu et al. 2010; Zhang et al. 2017). Negative SLP anomalies are predominant prior to and positive anomalies are predominant after the early 1990s. Compared to the pre-1990s period, the mean SLP over the Mongolian region increases by 1.5 hPa in the latter decade, which is close to its standard deviation. Associated with the increased MSLP, an inter-decadal change in the activity of regional extra-tropical cyclones is identified. There are significantly less and weaker summertime Mongolian cyclones during the post-1990s period.

Recent warming over EA may have an influence on the inter-decadal change in the MSLP, which features evident inhomogeneity in the spatial distribution. The most robust warming area is located in the Lake Baikal region, while much weaker temperature anomalies are observed over the adjacent Inner Mongolia Plateau. The meridionally-inhomogeneous air temperature anomaly distribution results in decreased lower-tropospheric south–north temperature

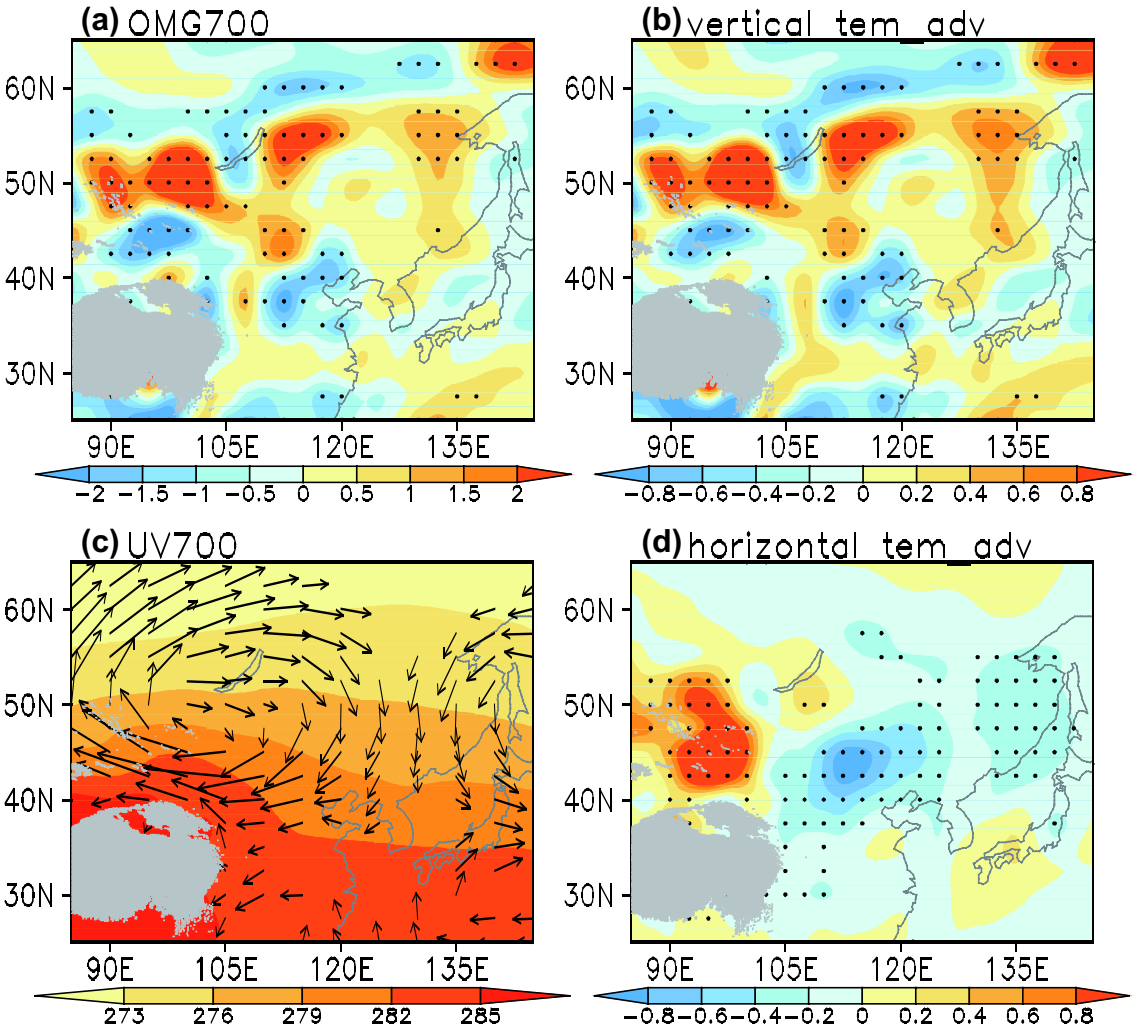

Fig. 10 **a** Difference of the 1991–2012 mean minus 1980–1990 mean summer **a** vertical p velocity (unit: 10^{-2} Pa s^{-1}), **b** vertical temperature advection (unit: 10^{-5} K s^{-1}), **c** horizontal winds (units: m s^{-1}) and **d** horizontal temperature advection (unit: 10^{-5} K s^{-1}) at 700 hPa. The black dots in **a, b** and **d** denote the differences exceeding the 95% confidence level based on the Student's t test. Color shadings in **c** denote the climatological 700-hPa air temperature (unit: K). Wind vectors are plotted only where the composite differences are statistically significant at the 95% confidence level by Student's t test

gradient, reduced vertical wind shear, and thus weakened atmospheric baroclinicity over the Mongolian region. Regional synoptic extra-tropical cyclones become less active in the presence of reduced baroclinicity in the later decade. As a macroscale manifestation, the decadal mean MSLP increases significantly.

The inhomogeneous warming may be partly attributed to the regional inhomogeneous distributions of cloud and radiation anomalies. Since the early 1990s, there are less cloud cover and more surface net solar radiation over the Lake Baikal region, while weak changes occur in the areas to the south. This external heating pattern favors the formation of meridionally-inhomogeneous temperature anomaly distribution. Further analyses find that the temperature anomaly structure is maintained by two positive feedback mechanisms associated with atmospheric internal processes. One mechanism is related to adiabatic heating. The decadal increased MSLP is accompanied by regional descent anomalies, with the strongest sinking around the Lake Baikal. Anomalous vertical warm temperature advection driven by the sinking is conducive to more rapid warming over the northern part, and thus maintains the decreased meridional temperature gradient between south and north of 45°N. The other mechanism is related to horizontal temperature advection. Associated with the inter-decadal increased MSLP, the dominant circulation anomalies are characterized by an anomalous lower-tropospheric anticyclone over NEA. Under the mean southwest–northeast temperature gradient, anomalous northeasterly winds prevailing on the southeast flank of the anticyclone cause anomalous cold advection over

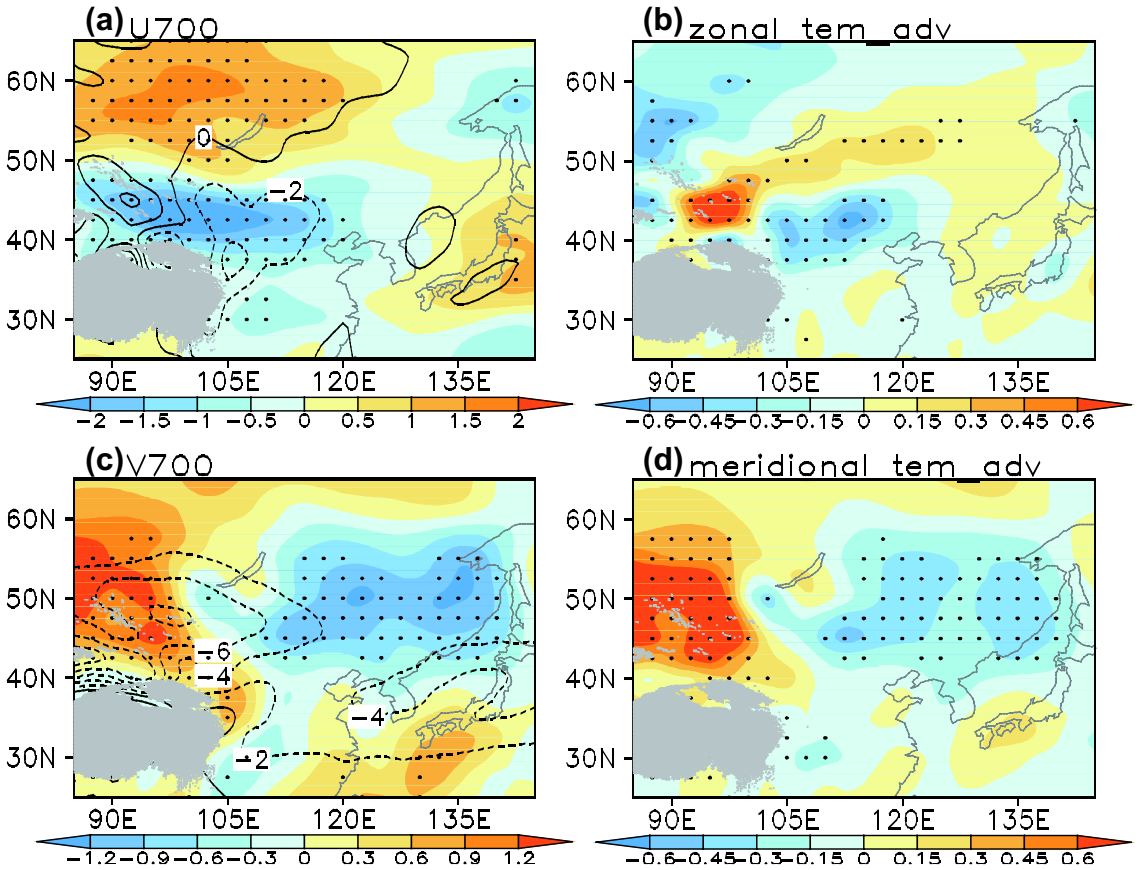

Fig. 11 **a** Difference of the 1991–2012 mean minus 1980–1990 mean summer **a** zonal wind velocity (shading, unit: m s^{-1}), **b** zonal temperature advection (unit: 10^{-5} K s^{-1}), **c** meridional wind velocity (shading, units: m s^{-1}) and **d** meridional temperature advection (unit: 10^{-5} K s^{-1}) at 700 hPa. Contours in **a, c** denote the climatological zonal and meridional temperature gradient (unit: 10^{-6} K m^{-1}) at 700 hPa, respectively. The black dots denote the differences exceeding the 95% confidence level based on the Student's t test

the Inner Mongolia Plateau south of 45°N. This anomalous horizontal cold advection acts against the anomalous adiabatic heating, and favors the development of meridionally-inhomogeneous temperature anomaly distribution.

The present study proposes a possible contribution of the inhomogeneous warming over NEA to the inter-decadal change in the MSLP. This is different from previous studies that highlighted the robust warming over the Lake Baikal region (Zhu et al. 2012; Du et al. 2016). In addition to the local factor, circulation anomalies over the polar region may have an influence on the SLP variations over Mongolia as a seesaw pattern between the two regions appears in all seasons, which is known as the Polar/Eurasia teleconnection (Barnston and Livezey 1987). The seesaw pattern seems to switch from a negative phase to a persistent positive phase around the end of 1980s (http://www.cpc.ncep.noaa.gov/data/teledoc/poleur.shtml), which might contribute to the decadal increased MSLP as well. Besides, some studies have documented that the inter-annual variations of atmospheric circulation over NEA could be affected by upstream thermal anomalies through teleconnections (Wu et al. 2009, 2011). Further study is needed to examine whether similar connections could be found on the inter-decadal timescale.

In the present analysis, we focus on exploring the mechanisms for the inter-decadal variation of the MSLP. Its impact on the EASM is not yet addressed. Wu et al. (2010) have highlighted the contribution of the anomalous anticyclone associated with the increased MSLP to the inter-decadal increase in southern China summer rainfall around the early 1990s. In addition, accompanying the change in the MSLP, intensity of the EASM weakens abruptly around 1990/1991 (Fig. 12a), which is due to the decreased zonal thermal contrast across EA according to Zhao and Zhou (2005). Particularly, summer southwesterly winds over North China and Northeast China reduce significantly (Figs. 10c, 12b), which may further affect regional weather and climate events. Different basic flows in different decades may provide different backgrounds for inter-annual variations. Accompanied by the increase in decadal mean MSLP, its inter-annual variability seems

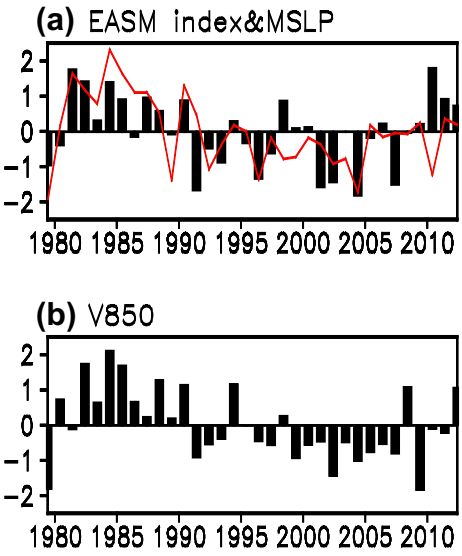

Fig. 12 Time series of the normalized **a** EASM intensity index from Zhao and Zhou (2005) and **b** 850-hPa meridional wind averaged over the region of 110°–130°E, 40°–50°N. The red curve in **a** denotes the MSLP anomaly index

to become weaker since the 1990s (Fig. 1d) with the year-to-year standard deviation reaching 1.3 hPa prior to 1990, but only 0.64 hPa after it. The mechanisms responsible for the weakening of inter-annual variability remain to be unraveled. Further study is needed to identify whether and how the change in inter-annual variability is associated with the background change in the early 1990s.

Acknowledgements This research was jointly supported by National Natural Science Foundation of China (41530503), National Key Basic Research and Development Projects of China (2016YFA0600601 and 2014CB953901), Research Projects of Public Welfare Meteorological Industry in China (201406001). RW acknowledges the support of National Natural Science Foundation of China grants (41530425 and 41475081).

References

Barnston AG, Livezey RE (1987) Classification, seasonality and persistence of low-frequency atmospheric circulation patterns. Mon Weather Rev 115:1083–1126

Chen SJ, Kuo YH et al (1991) Synoptic climatology of cyclogenesis over East Asia, 1958–1987. Mon Weather Rev 119:1407–1418

Chen LX, Zhu CW, Wang W et al (2001) Analysis of the characteristics of 30–60 day low-frequency oscillation over Asia during 1998 SCSMEX. Adv Atmos Sci 18:623–638

Chen JP et al (2015) Influences of northward propagating 25–90-day and quasi-biweekly oscillations on eastern China summer rainfall. Clim Dyn 45:105–124. https://doi.org/10.1007/s00382-014-2334-y

Chung YS, Dulam J (2004) Anticyclones over the territory of Mongolia. Asia Pac J Atmos Sci 40:317–329

Dee DP, Uppala SM, Simmons AJ et al (2011) The ERA-Interim reanalysis: configuration and performance of the data assimilation system. Q J R Meteorol Soc 137:553–597

Ding YH, Wang ZY, Sun Y (2008) Inter-decadal variation of the summer precipitation in East China and its association with decreasing Asian summer monsoon. Part I: observed evidences. Int J Climatol 28:1139–1161

Du MX, Lin ZD, Lu RY (2016) Inter-decadal change in the summertime Northeast Asia low-pressure system in the early 1990s. Chin J Atmos Sci 40:805–816 **(in Chinese)**

Duan AM, Wang MR et al (2013) Trends in summer rainfall over China associated with the Tibetan Plateau sensible heat source during 1980–2008. J Clim 26:261–275

Hoskins BJ, Valdes PJ (1990) On the existence of storm tracks. J Atmos Sci 47:1854–1864

Kanamitsu M, Ebisuzaki W et al (2002) NCEP-DOE AMIP-II reanalysis (R-2). Bull Am Meteor Soc 83:1631–1643

König W, Sausen R, Sielmann F (1993) Objective identification of cyclones in GCM simulations. J Clim 6:2217–2231

Lei YH, Hoskins B, Slingo J (2011) Exploring the interplay between natural decadal variability and anthropogenic climate change in summer rainfall over China. Part I: observational evidence. J Clim 24:4584–4599

Li SL, Bates G (2007) Influence of the Atlantic Multidecadal Oscillation on the winter climate of East China. Adv Atmos Sci 24:126–135

Lin ZD, Wang B (2016) Northern East Asian low and its impact on the interannual variation of East Asian summer rainfall. Clim Dyn 46:83–97. https://doi.org/10.1007/s00382-015-2570-9

Liu JT, Zheng XJ, Kang L et al (2003) A case study of a severe dust storm resulted from an explosive Mongolia cyclone. Clim Environ Res 8:218–229 **(in Chinese)**

Liu Y, Huang G, Huang RH (2011) Inter-decadal variability of summer rainfall in Eastern China detected by the Lepage test. Theor Appl Climatol 106:481–488

Lu R, Dong H, Su Q, Ding H (2014) The 30–60-day intraseasonal oscillations over the subtropical western North Pacific during the summer of 1998. Adv Atmos Sci 31:1–7

Magaritz M, Goodfriend GA (1987) Movement of the desert boundary in the Levant from latest Pleistocene to early Holocene. Abrupt climatic change. Springer Neth 216:173–183

Mao JY, Chan JC (2005) Intraseasonal variability of the South China Sea summer monsoon. J Clim 18:2388–2402

North GR, Bell TL et al (1982) Sampling errors in the estimation of empirical orthogonal functions. Mon Weather Rev 110:699–706

Qian W, Quan L, Shi S (2002) Variations of the dust storm in China and its climatic control. J Clim 15:1216–1229

Serreze MC (1995) Climatological aspects of cyclone development and decay in the Arctic. Atmos Ocean 33:1–23

Tao SY (1980) Storm rainfall in China. Science, Beijing, pp 91–146 **(in Chinese)**

Tao SY, Chen LX (1987) A review of recent research on the East Asian summer monsoon. In: Chang C-P, Krishnamurti TN (eds) China, Monsoon meteorology. Oxford University Press, Oxford, pp 60–92

Tong HW, Chan JCL, Zhou W (2009) The Role of MJO and Mid-latitude Fronts in the South China Sea Summer Monsoon Onset. Clim Dyn 33:827–841. https://doi.org/10.1007/s00382-008-0490-7

Ulbrich U, Leckebusch GC, Pinto JG (2009) Extra-tropical cyclones in the present and future climate: a review. Theor Appl Climatol 96:117–131

Wang SY, Chen TC (2008) Measuring East Asian summer monsoon rainfall contributions by different weather systems over Taiwan. J Appl Meteorol Clim 47:2068–2080

Wang H, Mehta VM (2008) Decadal variability of the Indo-Pacific warm pool and its association with atmospheric and oceanic

variability in the NCEP–NCAR and SODA reanalyses. J Clim 21:5545–5565
Wang XM, Zhai PM, Wang CC (2009) Variations in extratropical cyclone activity in northern East Asia. Adv Atmos Sci 26:471–479
Watts IEM (1969) Climates of China and Korea. In: Arakawa H (ed) Climates of northern and eastern Asia. Elsevier, Amsterdam, pp 1–77
Weng HY, Ashok K et al (2007) Impacts of recent El Niño Modoki on dry/wet conditions in the Pacific rim during boreal summer. Clim Dyn 29:113–129
Wu RS (2002) Contemporary principle of synoptic meteorology. Higher Education Press, Beijing, p 319 **(in Chinese)**
Wu BY, Zhang RH (2011) Interannual variability of the East Asian summer monsoon and its association with the anomalous atmospheric circulation over the mid-high latitudes and external forcing. Acta Meteorol Sin 69:219–233 **(in Chinese)**
Wu ZW, Wang B, Li JP et al (2009) An empirical seasonal prediction model of the east Asian summer monsoon using ENSO and NAO. J Geophys Res Atmos 114:d18120. https://doi.org/10.1029/2009JD011733
Wu RG, Wen ZP, Yang S, Li YQ (2010) An interdecadal change in southern China summer rainfall around 1992/93. J Clim 23:2389–2403
Wu RG, Yang S, Liu S et al (2011) Northeast China summer temperature and North Atlantic SST. J Geophys Res Atmos 116:971–978
Ye DZ, Zhu BZ (1958) Some fundamental problems of the general circulation of the atmosphere. Science, Beijing, p 159 **(in Chinese)**
Zhang SY (1989) The relation between cyclone activity and precipitation in spring in north China. Chin J Atmos Sci 13:247–251. https://doi.org/10.3878/j.issn.1006-9895.1989.02.15
Zhang YX, Ding YH, Li QP (2012) A climatology of extratropical cyclones over East Asia during 1958–2001. Acta Meteorol Sin 26:261–277
Zhang HY, Wen ZP, Wu RG et al (2017) Inter-decadal changes in the East Asian summer monsoon and associations with sea surface temperature anomaly in the South Indian Ocean. Clim Dyn 48:1125–1139
Zhao P, Zhou ZJ (2005) East Asian subtropical summer monsoon index and its relationships to rainfall. Acta Meteorol Sin 63:933–941 **(in Chinese)**
Zhou XJ et al (2003) Experimental study on storm rainfall in South China during 1998. China Meteorological Press, Beijing, p 215 **(in Chinese)**
Zhu QG, He JH, Wang PX (1986) A study of circulation differences between East Asian and Indian summer monsoons with their interaction. Adv Atmos Sci 3:466–477
Zhu CW, Wang B et al (2012) Recent weakening of northern East Asian summer monsoon: a possible response to global warming. Geophys Res Lett 39:278–283. https://doi.org/10.1029/2012GL051155
Zhu ZW, Li T, He JH (2014) Out-of-Phase relationship between boreal spring and summer decadal rainfall changes in southern China. J Clim 27:1083–1099